Climate and land-use changes interact to drive long-term reorganization of riverine fish communities globally

Lise Comte[a,b,1], Julian D. Olden[c], Pablo A. Tedesco[d], Albert Ruhi[e], and Xingli Giam[a,1]

[a]Department of Ecology and Evolutionary Biology, The University of Tennessee, Knoxville, TN 37996; [b]School of Biological Sciences, Illinois State University, Normal, IL 61790; [c]School of Aquatic and Fishery Sciences, University of Washington, Seattle, WA 98105; [d]Laboratoire Evolution et Diversité Biologique (EDB), UMR5174, Université Toulouse 3 Paul Sabatier, CNRS, Institut de Recherche pour le Développement (IRD), F-31062 Toulouse, France; and [e]Department of Environmental Science, Policy, and Management, University of California, Berkeley, CA 94720

Edited by Nils Chr. Stenseth, Universitetet i Oslo, Oslo, Norway, and approved May 13, 2021 (received for review June 5, 2020)

As climate change unfolds, changes in population dynamics and species distribution ranges are expected to fundamentally reshuffle communities worldwide. Yet, a comprehensive understanding of the mechanisms and extent of community reorganization remains elusive. This is particularly true in riverine systems, which are simultaneously exposed to changing temperature and streamflow, and where land-use change continues to be a major driver of biodiversity loss. Here, we use the most comprehensive compilation of fish abundance time series to date to provide a global synthesis of climate- and LU-induced effects on riverine biota with respect to changes in species thermal and streamflow affinities. We demonstrate that fish communities are increasingly dominated by thermophilic (warm-water) and limnophilic (slow-water) species. Despite being consistent with trends in water temperature and streamflow observed over recent decades, these community changes appear largely decoupled from each other and show wide spatial variation. We further reveal a synergy among climate- and land use-related drivers, such that community thermophilization is heightened in more human-modified systems. Importantly, communities in which species experience thermal and flow regimes that approach or exceed their tolerance thresholds (high community sensitivity), as well as species-poor communities (low community resilience), also display faster rates of compositional change. This research illustrates that quantifying vulnerability of riverine systems to climate change requires a broadening from a narrower thermal focus to more integrative approaches that account for the spatially varying and multifaceted sensitivity of riverine organisms to the interactive effects of water temperature, hydrology, and other anthropogenic changes.

climate vulnerability | community temperature index | community flow index | freshwater ecosystems | river fragmentation

Mounting evidence indicates that climate change is driving widespread community reorganizations (1, 2) and constitutes a leading threat to riverine biodiversity (3–5). This is problematic as flowing water ecosystems lie at the forefront of the current biodiversity crisis and are also among the most biodiverse on Earth (6). Studies point to the multifaceted nature of climate-induced effects in these ecosystems (7–9), emerging through alterations of both thermal and flow regimes globally (10, 11). Concurrently, land use remains a major and persistent driver of biodiversity loss in these ecosystems (4), whose long-lasting effects can mediate present-day biological responses to further environmental change (12). Recent calls have intensified to simultaneously explore the effects of thermal, hydrologic, and land-use drivers to strengthen our understanding and prediction of riverine biodiversity responses to climate change.

From a climate-change perspective, communities affected by greater climate exposure (characterized by the direction and magnitude of changes in water temperature and streamflow over time) are expected to display the fastest turnover rates (1, 2). This occurs through the gradual replacement of thermally and hydrologically sensitive species by species with broader temperature and flow affinities that colonize these newly climatically suitable areas from downstream reaches (4, 5, 13). It is also increasingly clear that climate change is not likely to act in isolation from other threats, and particularly so in human-dominated flowing water ecosystems (14). Human appropriation of land for agriculture and urban infrastructure, whose effects range from habitat loss, modified hydrology, riverscape fragmentation, alteration of riparian areas, to shifts in fluxes of energy and pollutants (15), can either amplify or dampen the effects of climate change. Removal of riparian vegetation may increase both incoming and outgoing radiation, leading to hotter, drier, and more variable thermal conditions than expected based on climate change alone (16). Interruptions of the river continuum or decreases in longitudinal connectivity may also limit species abilities to track their climatic niche through space, partially offsetting range expansion processes expected from climate change operating in isolation (17). An additional concern is that land use and climate change may indirectly select for species with the same suite of traits (e.g., pollution-tolerant species often also display warm-water affinities) (18), thus promoting faster community reorganizations (19,

Significance

Understanding the mechanisms by which biological communities are reorganized by environmental change is a key question facing ecologists. Using a global database of fish abundance time series spanning recent decades, together with community-level indices describing species temperature and flow affinities, we show that two important aspects of climate change (water temperature and streamflow alteration) are interacting with land-use modification to drive increases in the dominance of species that prefer warm- and slow-water habitats. Although these community reorganizations show substantial geographical variation, they can be explained by a combination of degree of environmental changes and initial community composition. These findings offer insights to improve ecological forecasting in the future to better inform and prioritize conservation actions in freshwater ecosystems.

Author contributions: L.C., J.D.O., P.A.T., A.R., and X.G. designed research; L.C. and X.G. performed research; L.C. analyzed data; and L.C., J.D.O., P.A.T., A.R., and X.G. wrote the paper.

The authors declare no competing interest.

This article is a PNAS Direct Submission.

[1]To whom correspondence may be addressed. Email: lccomte@ilstu.edu or xgiam@utk.edu.

This article contains supporting information online at https://www.pnas.org/lookup/suppl/doi:10.1073/pnas.2011639118/-/DCSupplemental.

Published June 21, 2021.

20). Land-use conversion can also decrease population size and genetic diversity, decreasing species ability to cope with other threats, including climate change (21). Although climate and land-use changes are perceived as self-reinforcing threats to biodiversity and human security (14, 22), their combined ecological effects remain unclear, which may limit our ability to establish conservation priorities at the local, regional, and continental scales (19).

Beyond extrinsic factors, the reshuffling of biological communities is also expected to be mediated by the intrinsic sensitivity and resilience (or adaptive) capacity of component species (23, 24). For instance, it is now recognized that the differences between local temperature regime and community-level temperature affinity (i.e., community thermal bias, sensu ref. 25) may ultimately determine the sensitivity of communities to warming. Similarly, community responses to climate-induced hydrologic alteration may be contingent on the differences between the flow affinity of constituent species and the flow regime they experience (i.e., community flow bias). Specifically, communities with low or negative values of thermal or flow bias (i.e., communities that are experiencing temperature or streamflow that is approaching or exceeding their preferred conditions) are expected to be more sensitive and exhibit greater scope for compositional changes in response to altered temperature or streamflow conditions. Theory also predicts that communities are more likely to be buffered against environmental change if constituent species exhibit a variety of traits that enable them to cope with the novel environmental regime (26, 27). Hence, high species richness is expected to increase community resilience to climate change through higher functional redundancy (28) and probability of containing climate-tolerant species (29). A host of other species characteristics can also be involved to determine species ability to cope with or adjust to changing environmental conditions (i.e., persist in place or shift in space) such as dispersal ability or demographic and genetic population attributes, collectively referred to as species adaptive capacity (23).

This study leveraged species abundance time series of riverine fish communities from monitoring programs and research projects around the world to quantify the effects of recent climate change, land use, and their interaction. We first quantified temporal changes in fish community composition with respect to the average affinity of species to both water temperature (community temperature index [CTI]) and streamflow (community flow index [CFI]). CTI has become a popular indicator of warming-induced biodiversity responses, where positive CTI trajectories indicate an increase in the dominance of warm-water (as opposed to cold water) species over time—a process termed thermophilization of communities (30–32).

Similar in concept, we introduce the CFI to describe temporal changes in community dynamics with respect to flow alterations. Although streamflow is generally higher in large lowland rivers compared to headwaters, rapid habitats (i.e., sections of a river where the river bed has a relatively steep gradient, high water velocity, and greater turbulence) are generally rare (33, 34). Hence, riverine fish community composition varies predictably along the longitudinal gradient, with upstream species better adapted to rapid habitats (rheophilic species) and downstream species to slow habitats (limnophilic species) (35). Positive CFI trajectories thus reflect an increase in the dominance of limnophilic (as opposed to rheophilic) species over time—a process referred to as limnophilization of communities.

We tested for directional trends in community trajectories by characterizing spatiotemporal patterns in CTI and CFI at global and ecoregion scales. Finally, we investigated possible drivers underlying variation in CTI and CFI trajectories among different communities. We predicted that climate exposure (temporal trends in water temperature and streamflow) (10) together with land-use change (i.e., agricultural and urban land use) interact synergistically to affect community trajectories in CTI and CFI. We also hypothesized that community intrinsic sensitivity (community thermal or flow bias) and community resilience capacity (species richness) mediate the rate of change in CTI and CFI. Acknowledging the inherent variability associated with secondary datasets collected for multiple purposes, we explicitly accounted for spatial dependencies and sampling unbalance among time series in all the steps of our analyses (*Materials and Methods*).

Results

The 12,517 time series of riverine fish communities span 10 to 68 y (average time span = 19 y; average number of census years = 8, range = 2 to 52; average first census year = 1996, range = 1951 to 2010; mainly using electrofishing techniques) and are distributed over five ecoregions and 446 hydrographic basins (*SI Appendix*, Fig. S1). The majority of the 102,285 annual surveys were conducted consistently in a single quarter or over two consecutive quarters through time (*SI Appendix*, Fig. S2). Of the 951 species included in the analysis, most occur in a single ecoregion (96%), with the highest total number of species observed in the Nearctic ($N_{Afrotropics}$ = 88; $N_{Australasia}$ = 88; $N_{Nearctic}$ = 493; $N_{Neotropics}$ = 191; $N_{Palearctic}$ = 141). However, we note clear spatial disparities in terms of global coverage, with a low (Afrotropical and Neotropical) or lack (Indo-Malayan) of sites in some of the most biodiverse ecoregions ($N_{Afrotropics}$ = 5; $N_{Australasia}$ = 506; $N_{Nearctic}$ = 2,317; $N_{Neotropics}$ = 76; $N_{Palearctic}$ = 9,613).

We found an overall thermophilization (52.3% of time series) and limnophilization (51.3% of time series) of riverine fish communities over recent decades (Figs. 1 and 2) according to water temperature (CTI) and streamflow (CFI) trajectories estimated from generalized least squares (GLS) models fitted separately to each time series, respectively (*Materials and Methods*). Despite these general trends, these community trajectories (CTI and CFI) vary widely and are uncorrelated at the global scale (r = 0.04; see also *SI Appendix*, Figs. S3 and S4). Whereas one-third of the time series show an increase in the dominance of warm-water and limnophilic species (33.1%), shifts toward cold-water and rheophilic species (26.4%), warm-water and rheophilic species (19.2%), or cold-water and limnophilic species (18.2%) are also commonly observed. No change in either CTI or CFI was detected in 2.8% of the communities.

These findings are consistent between occurrence- and abundance-based community metrics (*SI Appendix*, Fig. S5), indicating that changes in CTI and CFI did not only result from changes in species abundance distributions but also from changes in species turnover. Moreover, these results are robust to alternate

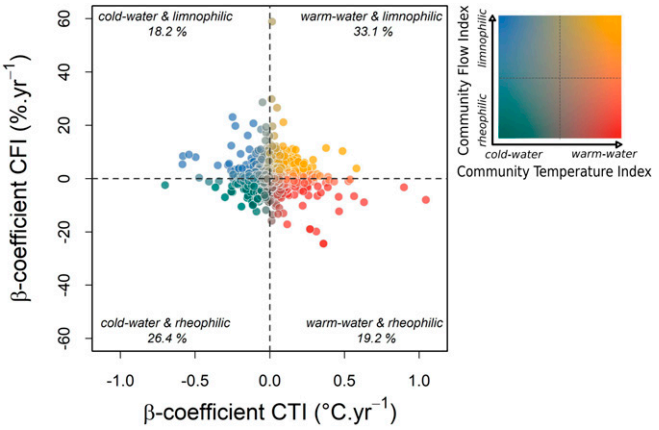

Fig. 1. Temporal trajectories of fish communities. Comparison of the trajectories (β-coefficient) in CTI and CFI indicates the direction of the changes in community composition over time in terms of species temperature gradient (from cold to warm water) and streamflow (gradient from rheophilic to limnophilic) affinities as illustrated by the color legend.

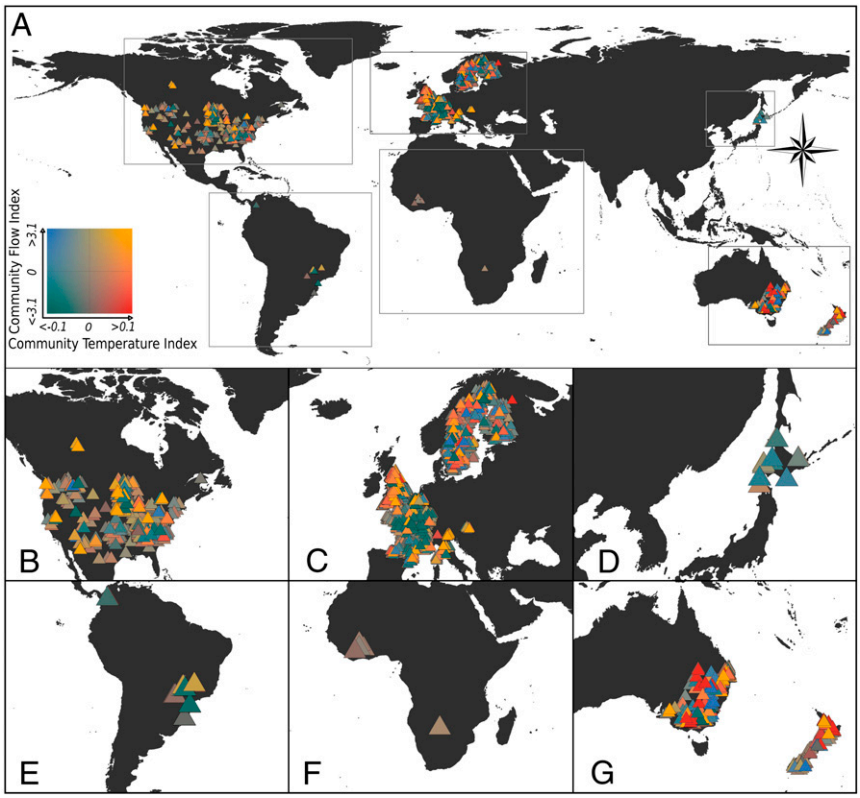

Fig. 2. Maps of the community trajectories in CTI and CFI illustrated at the (*A*) global scale and in (*B*–*G*) selected areas. Each triangle represents a time series; its color indicates the direction and magnitude of changes, expressed in °C·y^{-1} and %·y^{-1}, respectively.

estimations of species temperature (species temperature index [STI]) and streamflow (species flow index, SFI) affinities. Indeed, our distribution-based STI (i.e., based on the median instead of 95th percentile of species distribution along environmental gradients and the mean annual temperature instead of the maximum monthly annual temperature) was the most correlated with temperature preferences derived from physiological experiments (r = 0.78; $N_{species}$ = 580; *SI Appendix*, Fig. S6), and that using alternative formulas accounted for less than 1% of the total variability in the CTI and CFI trajectories (*SI Appendix*, Table S1). In addition, although the range coverage of the occurrence datasets used to estimate STI (using the International Union for Conservation of Nature [IUCN] range maps as reference) varied among species (mean = 57%; range = 0.5 to 100%; $N_{species}$ = 586), there was no systematic bias in comparisons between distribution-based STI estimates and physiology-based temperature affinities across the coverage gradient (t value = −0.49, P = 0.628; $N_{species}$ = 484; *SI Appendix*, Fig. S7).

Lastly, we found little evidence that variability in the time series characteristics (i.e., sampling quarter consistency and number of census years) was associated with a directional bias in the CTI or CFI trajectories (*SI Appendix*, Fig. S8). However, we note that despite our efforts, the quarter of sampling displayed a small directional trend over time, with the most recent surveys being performed earlier in the year compared to the oldest ones (linear regression coefficient = -1.19×10^{-3}, equivalent to a mean shift of −0.0119 to −0.081 quarters over the range of study durations; t value = −4.27, $P < 0.001$ for all surveys). No temporal trend was found with regards to the sampling month (t value = −1.07, P = 0.284 for 98,312 surveys for which this information was available), supporting the finding above that shifts in sampling window are minimal, and indicating that it is unlikely to affect our conclusions. If these small shifts in sampling window did result in community composition changes, our documented rates of community reorganization will be conservative estimates as most recent surveys are collected earlier in the year when stream temperatures are lower.

We found that CTI has increased globally with a mean rate of thermophilization of 0.003 °C·y^{-1} (95% CI = 0.001–0.005; Fig. 3*A*) according to linear mixed models that accounted for spatial dependencies (i.e., due to shared environmental conditions and species dispersal among sites within the same hydrographic basin) and sampling imbalance (i.e., the fact that the precision of the estimates increases with sample size) among the time series (*Materials and Methods*). Despite positive trends in all ecoregions, these increases are significant only for Australasia (0.019 °C·y^{-1}; 95% CI = 0.011–0.026), with the highest degree of uncertainty found for Afrotropics and Neotropics that are also the ecoregions with the smallest sample sizes. No significant spatial pattern was identified with respect to stream order (linear effect: t value = 0.09, P = 0.932; quadratic effect: t value = 0.21, P = 0.831), indicating that both increases and decreases are observed irrespective of site location along the longitudinal stream gradient (Fig. 3*B*).

An increase in CFI is also evident globally, with a mean rate of limnophilization of 0.07%·y^{-1} (95% CI = 0.02–0.13). However, both significant increases and decreases are observed at the ecoregion scale where estimates range from −1.31%·y^{-1} (95% CI = −1.97 to −0.66) for Neotropics to 0.08%·y^{-1} (95% CI = 0.02 to 0.14) for Palearctic (Fig. 3*C*). Again, Afrotropics and Neotropics show the highest degree of uncertainty. Changes in CFI are also nonrandomly distributed along the longitudinal stream gradient (linear effect: -1.59×10^{-3}, t value = −4.31, $P <$ 0.001; quadratic effect: 3.40×10^{-4}, t value = 6.29, $P < 0.001$), with the highest rates of limnophilization found for sites located on higher stream orders (Fig. 3*D*).

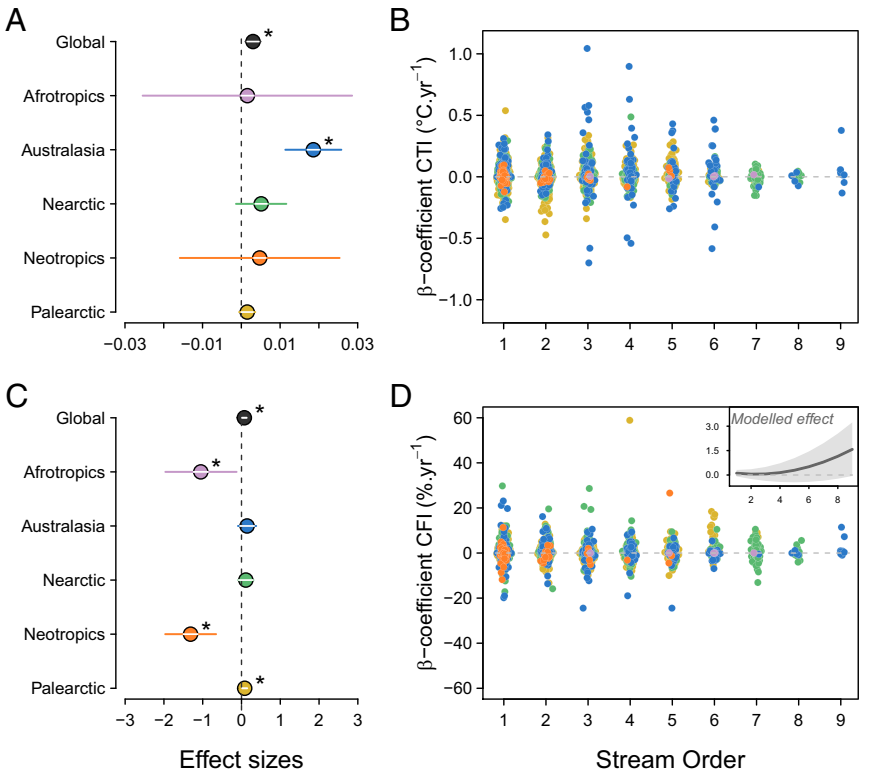

Fig. 3. Spatial patterns in CTI and CFI trajectories. (*A–C*) Global and ecoregion temporal trajectories (effect sizes) in (*A*) CTI and (*C*) CFI where error bars represent the 95% confidence intervals and asterisks indicate confidence intervals that do not cross zero. (*B–D*) Longitudinal patterns in the temporal trajectories in (*B*) CTI and (*D*) CFI (β-coefficient) according to stream order, where each dot represents a time series. Colors indicate the ecoregions as defined in *A–C* and dots have been jittered for clarity. The gray line and shaded area in the *Inset* in *D* illustrate the modeled effect and associated 95% confidence interval.

Changes in CTI and CFI are best explained by a combination of climate- and land use-related drivers, as well as intrinsic community properties (Fig. 4) based on the results of a model averaging procedure involving top Akaike Information Criterion corrected for small sample size [AICc]-ranked models (ΔAICc ≤ 4; see *SI Appendix*, Table S2 for the results of the full models). CTI and CFI trajectories are positively associated with climate exposure in terms of the rate of increase in maximum average monthly water temperature (T_{max}) and streamflow (Q_{max}). Communities that experienced higher rates of increase in temperature and flow tend to show steeper trajectories toward thermophilization and limnophilization, respectively. Noteworthy, our climate exposure metrics are significantly and positively associated with trends derived from in situ measurements of both water temperature (linear regression coefficient = 0.10; t value = 2.39, $P = 0.019$; $N_{sites} = 84$) and streamflow (linear regression coefficient = 0.49; t value = 4.97, $P < 0.001$; $N_{sites} = 48$). This indicates that our metrics, which are calculated from coarse-resolution environmental time series (resolution ∼10 km), reasonably represent the environmental changes that occurred at the study sites (*SI Appendix*, Fig. S9). Land use also appears as an important driver and interacts with climate exposure in explaining CTI trajectories. Land use and trends in T_{max} have a comparable effect on the rates of community reorganization and show synergetic interactions, such that the increase in CTI (thermophilization) is higher in human-modified than in more natural systems under similar rates of increase in T_{max} (Fig. 5*A*). A similar but nonsignificant effect is observed for CFI, indicating that limnophilization of riverine fish communities likely occur independently from the gradient of land use (Fig. 5*D*).

In addition to the degree of exposure to environmental change, thermal bias and flow bias are the best predictors of CTI and CFI trajectories, respectively. Specifically, the rates of change in CTI and CFI are greater at sites in which starting communities have experienced temperature and streamflow that were close to or exceeded their average preferences (i.e., low or negative values of thermal bias and flow bias). Thermal bias and flow bias also interact with climate exposure, such as climate change responses are mediated by community intrinsic sensitivity. The interaction between thermal bias and the trends in T_{max} indicates that the most temperature-sensitive communities (with low thermal bias) tend to display high rates of CTI increases irrespective of the magnitude of climate exposure (Fig. 5*B*). The intrinsic sensitivity of communities is then gradually less important in determining CTI trajectories as the trends in T_{max} intensify. By contrast, the interaction between flow bias and the trends in Q_{max} indicates that the highest rates of CFI changes are observed only when both climate exposure and community intrinsic sensitivity are high (Fig. 5*E*). CFI trajectories are positively correlated with Q_{max} trends in the most flow-sensitive communities (with low flow bias), but the relationship lessens as flow bias decreases. In accordance with the effects of diversity on the resilience capacity of communities, we also identified a significant effect of species richness on both CTI and CFI trajectories, where species-poor communities show the greatest rates of change (Fig. 5 *C–F*).

Discussion

We provide a global synthesis of temporal trends in fish biodiversity in response to ongoing environmental changes in flowing water ecosystems. Our findings demonstrate an overall fingerprint of recent climate-induced changes in water temperature

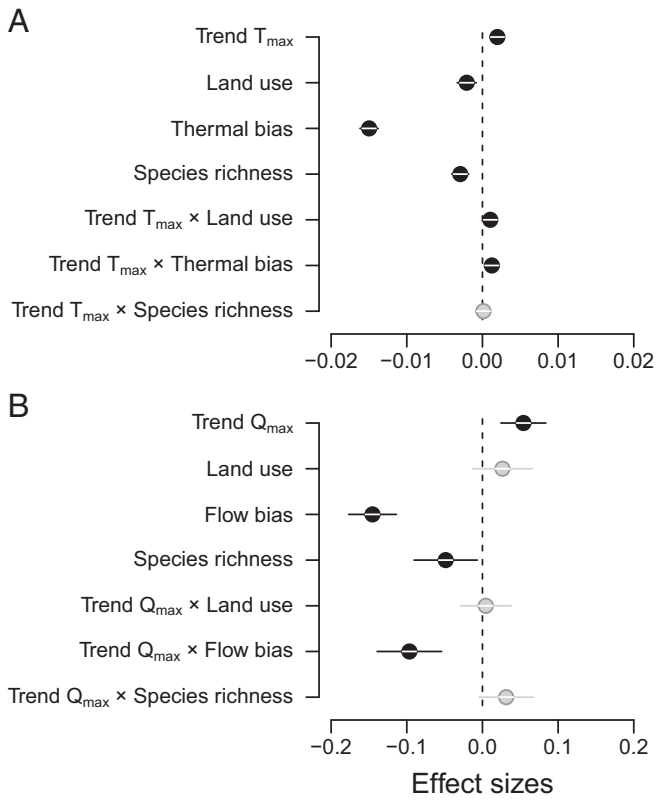

Fig. 4. Drivers of fish community trajectories. Direction and magnitude of the effect of climate exposure (trends in maximum average monthly temperature [T_{max}] or streamflow [Q_{max}]), land use, community sensitivity (thermal bias or flow bias), community resilience capacity (species richness), and their interaction (effect sizes) on (*A*) CTI and (*B*) CFI trajectories. Error bars show the 95% confidence intervals where darker dots indicate confidence intervals that do not cross zero.

and streamflow on riverine fish communities, but concurrently highlight the varied and complex pathways by which climate exposure interacts with land-use changes and intrinsic community properties to reshuffle communities. Acknowledging the spatially varying and multifaceted responses of riverine communities to climate and land-use changes is thus crucial to develop reliable forecasts to support adaptive management strategies in these ecosystems.

We show that the increasing dominance of warm-water (thermophilization) and slow-water (limnophilization) species in fish communities are widespread phenomena across a range of geographical and environmental contexts, where they manifest as a result of changes in maximum water temperature and streamflow. The global increase in CTI of 0.003 °C·y^{-1} is substantially lower than the rates documented for marine fishes based on commercial catch (0.02 °C·y^{-1}) (31), but higher than for other freshwater organisms such as invertebrates (0.001 °C·y^{-1}) (13). This may reflect the dual effects of stronger physical constraints on species (re)distribution in riverine than marine systems and the existence of resistance strategies in many aquatic invertebrates (i.e., desiccation-resistant forms) (36). However, when analyzed separately for different ecoregions of the world, we found that only Australasia displays an overall significant trend toward thermophilization, similar to the rates observed for marine fish communities (31). In addition, no clear spatial structuring was evident along the longitudinal stream network. This indicates a high degree of context dependency in fish community responses to changes in thermal conditions owing to opposing longitudinal gradients in extrinsic environmental drivers and intrinsic community sensitivity and resilience capacity. Specifically, the distribution of the extrinsic and intrinsic drivers of change along the longitudinal gradient suggests that whereas fish communities located in low order headwater streams show a greater scope for composition changes because they display the lowest thermal bias (higher sensitivity) and species richness (lower resilience capacity), the highest degree of exposure to warming and land-use changes have so far occurred in higher order streams (*SI Appendix*, Fig. S10). Given the observed relationship between community reorganization and the direction and magnitude of climate exposure, we therefore expect a higher proportion of communities to shift toward warm-water dominance as water temperatures warm into the future (4, 5).

We also found an overall tendency for communities to become more limnophilic (0.07%·y^{-1}). The direction and magnitude of the changes again exhibit considerable geographic variation, both among and within ecoregions, mirroring the complex patterns of positive (e.g., northern high-latitude rivers, northeastern United States) and negative (e.g., lower and midlatitudes, southern and western United States) climate-induced trends in streamflow previously reported among river basins (e.g., refs. 11, 37). Notably, these community changes also display spatial structuring along the longitudinal stream gradient (within river basins), with the highest rates of limnophilization observed in communities located in medium to large stream orders, that also display the highest degree of exposure to altered streamflow and community sensitivity (*SI Appendix*, Fig. S10). This is congruent with the predicted upstream shift of species distributions along riverine networks from the most downstream habitats (38), but also calls for a better understanding of the effects of river fragmentation on species expansions to smaller order tributaries (39). Taken together, our findings indicate that climate-induced alteration in water temperature and streamflow (and subsequent impacts on riverine biota) can be largely decoupled at a variety of local to regional scales. A better integration of these two essential facets of climate-induced change would enhance the realism of ecological forecasts into the future.

Most importantly, our results demonstrate synergies among climate- and land-use–related drivers of change, adding to the growing body of evidence that an emphasis on climate only—through temperature change—could impede our ability to anticipate biodiversity trends in the future (9, 39, 40). Notably, we show that the effects of climate exposure on CTI are exacerbated in systems with high levels of land use. This can be explained by three nonmutually exclusive factors: 1) water temperature increases due to removal of riparian vegetation and stormwater runoff from impervious surfaces not captured by the water temperature simulation model used (see ref. 10 for details), 2) reduced community resilience beyond changes in species richness and composition (e.g., intraspecific phenotypic and genetic diversity) (21), and 3) trait-based community filtering toward human-affiliated species tolerant of greater climatic variation (19, 20).

By contrast, our study shows the dominant effects of recent changes in streamflow on community composition, regardless of the land-use context. This result may be partially explained by the fact that human-induced hydrological changes such as dams, water withdrawals, and irrigation are already accounted for in the hydrological model (see ref. 41 for details). Nonetheless, this confirms that climate signals are not likely to be obscured by direct human influences on flow regimes (11, 37). Although methods have been proposed to control for the effects of different drivers of change on community trajectories (42), we argue that quantifying their potential synergies (or lack thereof) in nature allows for more realistic, though potentially more concerning, assessments of future threats to riverine fish biodiversity.

Beyond changes in water temperature, streamflow, and land use, the effects of climate exposure on community composition are mediated by the interplay with community intrinsic sensitivity

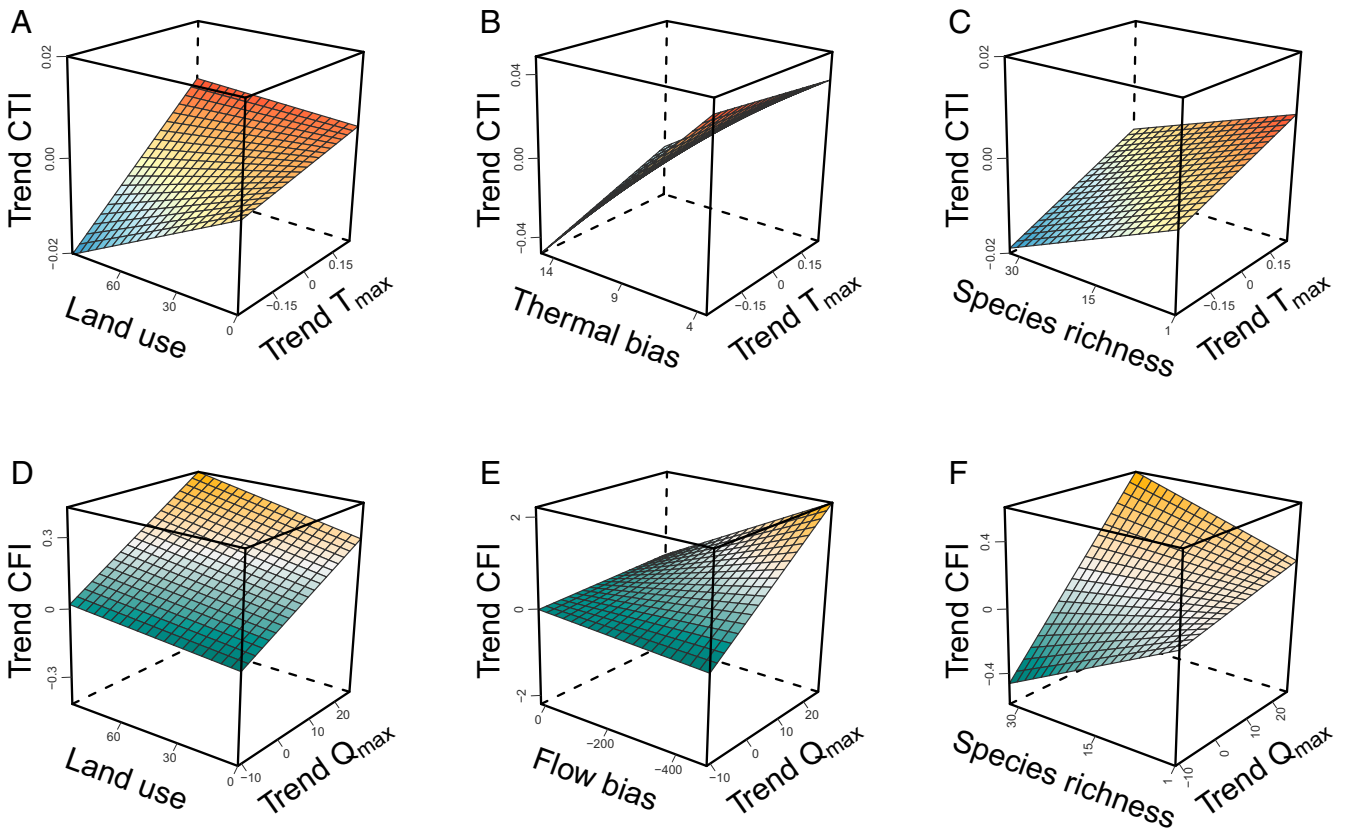

Fig. 5. Modeled interactions between drivers of fish community trajectories. (*A–C*) CTI (in °C·y^{-1}) and (*D–F*) CFI (in %·y^{-1}) trajectories as a function of the interaction between climate exposure (trends in maximum average monthly temperature [T_{max} in °C·y^{-1}]) or streamflow [Q_{max} in %·y^{-1}]) and (*A–D*) land use (in %), (*B–E*) community sensitivity (thermal bias in °C or flow bias in m^3·s^{-1}), and (*C–F*) community resilience capacity (species richness). Predictions were derived over the 1st to 99th percentile range observed for the predictor variables.

and resilience capacity. As expected, we find that the match between species niches and experienced environmental regimes (community thermal or flow bias) is a fundamental determinant of biodiversity responses to climate change (25, 27), where the most sensitive communities also display the highest rates of species reorganization. Interestingly, among the most thermally sensitive communities, the rate of thermophilization is high, irrespective of warming trends. This result is intuitive because communities at sites that are experiencing water temperatures that are already close to (or higher than) those preferred by species are also expected to experience declines in abundance and/or a turnover toward species adapted to warmer waters. As a result, changes in fish community are more likely to reflect recent climate exposure when the initial community is less thermally sensitive. Contrastingly, changes in streamflow have the greatest effect on limnophilization in the most flow-sensitive communities. In less flow-sensitive communities, trends in streamflow result in little to moderate change in the community with respect to its flow preference. Together, these results suggest that effects of recent warming are more profound and present a greater threat to riverine fish communities than recent flow alterations because all communities regardless of their temperature sensitivity were greatly reorganized at the highest levels of water temperature increase. This lends support to the forecast that the vulnerability of riverine fishes will be increasingly determined by climate warming exposure in the future (43).

We also provide evidence of the buffering effect of species diversity on the rate of community reorganization, confirming that the initial state of communities can effectively increase community resilience to environmental change (28). Although more sophisticated community properties such as temporal stability (32), functional redundancy (29), or thermal diversity (27) would undoubtedly provide more mechanistic explanations of the observed patterns, species richness as used in our analysis offers a simple tool for measuring climatic susceptibility that is easily transferable across systems and taxonomic groups. In turn, our findings suggest that the general expectation that climate change favors warm-water species may be too simplistic in riverine systems. Freshwater fish faunas are uniquely susceptible to environmental change because of the same factors that gave rise to their extremely high degree of endemism and biodiversity—the fact that their movement is constrained by the branching structure of stream networks and isolation within river basins. This results in limited redistribution opportunities but also strong longitudinal and regional variation in community intrinsic properties such as warming tolerance and species richness (44, 45).

The global assessment of community compositional trends in riverine fishes presented here is based on the most comprehensive compilation of fish abundance time series to date. This unique dataset allows us to draw crucial conclusions concerning the recent fingerprint of climate change on an ecologically, commercially, and culturally important vertebrate group worldwide. Despite the global scope of our study, we note clear disparities in terms of geographic coverage of available data, with relatively few data points in tropical river basins (e.g., no sites in the Amazon or Mekong basins). Because these basins harbor exceptional diversity in fish (44) that live closer to their thermal

limits (43, 46), the underrepresentation of tropical areas currently preclude a complete understanding of climate-induced community reshuffling in flowing water ecosystems. Given that different regions of the world may also display distinct patterns of overlap among anthropogenic drivers (47), with some of the fastest changes in land cover on the planet recorded in the tropics (48), these spatial biases may limit a fuller understanding of biodiversity change drivers (including the potential for interactive effects), and thus our ability to implement appropriate climate-change adaptive management strategies (49). Consequently, further research in these comparatively understudied biodiversity hotspots is urgently required (46, 48). Acknowledging the inherent limits of broad-scale biodiversity analyses such as ours (e.g., distribution-based estimates of thermal affinities, variation in the timing of surveys over time, resolution of environmental time series), we hope this study will stimulate future research, ideally examining other facets of community dynamics (e.g., taxonomic and trait diversity) (50), as well as assessing the consequences of changes in variability (instead of average) in temperature and flow regimes (51, 52).

Materials and Methods

Fish Abundance Data. Time series of fish abundance estimates were obtained from a global database of riverine fish community time series (RivFishTIME) (53), completed by additional national, state, and regional monitoring programs (see *SI Appendix*, Table S3 for a full list of the datasets used). Following RivFishTIME, time series were included if 1) the sampling methods were reported and consistent through time, 2) the sampling protocol was designed to target the entire fish community (i.e., as opposed to species-specific surveys), 3) the precise location (i.e., geographical coordinates) was available, 4) the time span was at least 10 y, and 5) two or more census years were available. We further excluded time series with null abundances, removed records involving non–ray-finned fishes (e.g., lampreys) or unidentified species from time series, and harmonized the taxonomy at the species level according to Fishbase (54). The geographical coordinates of the sites were used to assign each time series to an ecoregion (Afrotropic, Australasia, Nearctic, Neotropic, and Palearctic) and hydrographic basin (HydroSHEDS) (55), as well as to extract environmental data (see below). We also assigned a Strahler stream order to each time series by spatially snapping the sites to the RiverATLAS network (56) using a 500-m buffer (i.e., sites located within 500 m of the river network were assigned the stream order of the closest stream segment; 23% of the sites located farther away were assigned missing values). Time series collected at the same sites but using different sampling methods were considered separately in the analyses. Although limited in extent (i.e., fewer than 14% of the time series include multiple sampling events within a given year), we included only one sampling event per year to avoid temporal pseudoreplication in our analysis. To reduce potential sampling biases, we favored surveys performed in the same quarter of the year (1: January–March; 2: April–June; 3: July–September; and 4: October–December), and when this information was available in the same month within the same quarter. To test for potential directional trend in the temporal characteristics of the surveys, we used linear mixed models specifying either the sampling quarter or sampling month as response variable, year as a fixed effect, and time series identifier (ID) as a random effect on the intercept.

Environmental Data. We obtained water temperature (57) and streamflow (58) monthly time series for the period 1979 to 2014 at a 5-arc minute (~10 km) resolution at the global scale. Briefly, these datasets were simulated using the dynamical one-dimensional (1-D) water energy routing model (DynWat), that solves both the energy and water balance at the daily timestep. Although location-specific water temperature and streamflow time series were not available for most of the sampled sites, the DynWat model accounts for various anthropogenic (e.g., water abstraction, reservoir operations) and natural (e.g., ice breakup, flooding) processes, enabling a realistic representation of water temperature and flow regimes at a fine spatiotemporal scale (see refs. 10, 41 for more details). Despite being able to produce accurate estimates of daily discharge and temperature, it is important to note that the hydrologic model includes human–water interactions, whereas the water temperature simulations do not account for direct human impacts on temperature regimes (e.g., anthropogenic heat effluent or increase incoming radiation due to removal of riparian vegetation).

Using these environmental time series, we estimated climate exposure using the temporal trends in maximum average monthly water temperature (trend T_{max}; $°C \cdot y^{-1}$) and streamflow (trend Q_{max}; $\% \cdot y^{-1}$). These were quantified independently for each time series based on the fitted slope of a GLS model based on the yearly values in T_{max} or (*ln* transformed) Q_{max} with year as a predictor variable. The models were fit on the period covered by each time series minus the last census year, but including the 4 y prior to the first census year to account for long-term antecedent effects on fish recruitment success (59, 60). When the first and last census years were prior to 1983 and after 2015, respectively, the time window used to compute the temporal trends in water temperature and streamflow was dictated by data availability in the time series (median number of missing years across all time series = 1). To ensure temporal representativeness of climate exposure and convergence of the models, we kept only time series with at least 8 y of data.

To assess the ability of these coarse-resolution environmental time series to capture local environmental changes, we compared the metrics of climate exposure to trends estimated from in situ measurements of water temperature and streamflow. Observed water temperature trends were estimated based on water temperature measurements recorded during the fish community surveys for a subset of sites for which this information was available for at least 8 y within the same quarter of the year (T_{field}; N_{sites} = 84). Observed streamflow trends were estimated using maximum monthly average values based on daily gauge measurements accessed through the Global Runoff Data Center (available at https://www.bafg.de/GRDC/EN/Home/homepage_node.html). To do so, we selected gauges that were located within 200 m of the studied sites and for which measurements covered at least 8 y within the same temporal window, after discarding years with more than 75% of missing daily measurements (Q_{field}; N_{sites} = 48). Similar to modeled environmental time series, these trends were estimated independently for each observed time series based on the fitted slope of a GLS model based on the yearly values in T_{field} or (*ln* transformed) Q_{field} with year as a predictor variable. We then compared modeled to observed environmental trends using linear regressions.

Land cover data were obtained through the GlobCover2009 database that provides land cover classes values at a 300-m resolution for the year 2009 (61). Land use was then estimated as the percentage of cells within a 25-km buffer classified as croplands, artificial surfaces, and associated urban areas (i.e., corresponding to classes #11, #14, #20, #190, and #200). For practical purposes, we used a snapshot instead of dynamic land-use changes as most of the changes from natural to human land uses likely occurred before the last decades (our study period) and that no historical land cover dataset was available (or reliable) at a fine spatiotemporal scale (62). Nonetheless, we recognize that land cover is not truly static, and that land conversion undoubtedly occurred, which might have affected our results.

Trajectories in Community Temperature and Streamflow Affinities. Community temporal trajectories were estimated in terms of 1) species temperature (a gradient of cold to warm water) and 2) streamflow (a gradient from rheophilic to limnophilic) affinities using the CTI and CFI, respectively (30, 32). CTI and CFI summarize the average temperature and flow preferences of all species present at a given year at each site (i.e., community).

We estimated the STI and SFI indices for each of the 951 species recorded in the time series. We used long-term (1981 to 2010) mean annual water temperature (°C) and streamflow ($m^3 \cdot s^{-1}$) aggregated at a 2.5-arc minute (~25 km) resolution and species occurrences gathered from the Global Biodiversity Information Facility (63). We removed fossil specimen records, records of unknown origin, literature-based records with no specimens, records of specimens collected before 1975, and we removed duplicates. We also identified erroneous coordinates (based on the match between the recorded country and the country extracted from the geographical coordinates) and removed records that did not overlap with the presence of water (based on the GloRiC database) (64). To limit the influence of spatial biases in the biodiversity records (i.e., patchiness of collection effort), occurrence records were aggregated to a 2.5-arc minute (~25 km) resolution. Indeed, even for well-sampled species, occurrences are often clustered around areas of high accessibility or areas of management interest, making it difficult to distinguish between locations where the species is absent from sampling gaps across its distribution. As such, increasing the spatial grain reduces the number of cells with little-to-no sampling, and thus the potential for false absences (65). The STI and SFI were then computed as the median temperature and streamflow value within a species range (median among all 2.5-arc minute grid cells occupied by the species) (e.g., refs. 18, 30).

Because these indices could be estimated using slightly different formulas (e.g., ref. 32), we compared alternative STI estimates (i.e., using the 95th percentile value of mean annual temperature instead of the median or using

the maximum monthly instead of mean temperature) with temperature preferences derived from physiological experiments (43) for more than half of the number of species included in our study (i.e., those species with data from physiological experiments; $N_{species}$ = 581). We also assessed the influence of these methodological choices on the final community trajectories based on the percentage of variance explained by the type of biological data (abundances versus occurrences), distributional parameter (median versus 95th percentile), and environmental variables (mean annual versus maximum average monthly) with respect to the total variance estimated using linear regressions.

To assess the representativeness of the occurrence datasets with respect to species distributions, we also estimated the percentage of range coverage using the IUCN range maps as reference (66). To be able to compare the IUCN range maps—based on river catchments—with point occurrences, we calculated the ratio between the total area covered by the IUCN range maps (i.e., sum of the areas covered by all river catchments), and the area of the river catchments covered by the occurrence datasets (i.e., sum of the areas of all the river catchments where at least one occurrence was selected in the final dataset), which we further expressed in percentage (range coverage, %). Due to limited availability of IUCN range maps for the species included in our study, this analysis was restricted to 586 fish species (of the 951 species in our community time series dataset). We further assessed whether the degree of range coverage introduced potential biases in the estimations of the distribution-based temperature affinities. To do so, we calculated the ratio between the STIs and the physiology-based temperature affinities (CT_{max}) for the species for which this information was available ($N_{species}$ = 484), and tested the association between this ratio and range coverage using a linear regression.

Next, we computed the CTI and CFI for each time series-by-year combination as the mean STI and SFI across all the recorded species in each community in each year, weighted by their (*log* transformed) abundances. We used *log*-transformed abundances to reduce the influence of stochastic fluctuations and sample errors in the counts of high-abundant species (67). We also excluded CTI or CFI estimates of a given community from our analyses when more than 25% of the species in that community were missing STI or SFI due to a lack of occurrence data.

Last, we estimated temporal trajectories in CTI and CFI using GLS models, including CTI or CFI as response variables (CFI was *ln* transformed to reduce skewness) and year as a predictor. The temporal trajectories in CTI and CFI for each time series were then estimated using the slope coefficient (β-coefficient) expressed in $°C{\cdot}y^{-1}$ and $ln[m^3{\cdot}s^{-1}]\ {\cdot}y^{-1}$, respectively. Note, however, that to facilitate interpretability of the β-coefficients from the *ln*-linear models, we expressed the trajectories in CFI in $\%{\cdot}y^{-1}$ using the back transformation $(e^{\beta} - 1) \times 100$ (untransformed values are presented in *SI Appendix*). Whereas an increase in CTI indicates an increase in the representation of warm-water species (high STI) at the expense of cold-water species (low STI), an increase in CFI indicates an increase in the dominance of limnophilic species (downstream species with high SFI) at the expense of rheophilic species (upstream species with low SFI).

Community Characteristics. We estimated community intrinsic sensitivity to climate exposure through community thermal bias (25) or flow bias, which quantifies the difference between the community thermal or streamflow affinity and the thermal and flow conditions experienced by the community at the start of the time series. To do so, we calculated for the first census year of each time series the difference between STI or SFI and the long-term (1981 to 2010) mean annual water temperature (°C) and streamflow ($m^3{\cdot}s^{-1}$) aggregated at a 2.5-arc minute (~25 km) resolution, averaged across species and weighted by the species (*log* transformed) abundances. Communities with negative or low positive thermal bias or flow bias values are likely more affected (i.e., sensitive) by temperature or flow increases because they are experiencing temperatures or flows that already exceed or are about to exceed conditions preferred by their constituent species. Conversely, a large positive thermal bias or flow bias value indicates that species in the community on average prefer temperature or flow that is much higher than conditions they are experiencing; therefore, the community is likely less sensitive to alterations in temperature or flow conditions. We also estimated community resilience capacity through species richness, using the number of species recorded during the first census year.

Spatial Patterns in Community Trajectories. Spatial patterns in CTI and CFI trajectories were assessed at the global, ecoregion, and site (along the longitudinal stream gradient) scales. To do so, we first built a linear mixed effects model (68) with CTI or CFI trajectory as the response variable (β-coefficient in CTI or CFI) without any covariate to estimate the direction and magnitude of the global trend in CTI or CFI (effect size). We then fit the same models but adding ecoregion as a fixed effect and removed the global intercept to obtain one estimate per ecoregion. Lastly, we examined the longitudinal gradient patterns in CTI or CFI using stream order as a fixed effect in the models. We included both linear and quadratic terms to account for potential nonlinear community responses along the longitudinal stream gradient. To account for spatial autocorrelation among the time series due to shared environmental conditions and species dispersal among sites, we specified the hydrographic basin ID as a random effect on the intercept in all the models. We also included the number of census years as weight (sampling weights) to control for the effect of unequal sample size among the time series (i.e., the fact that the precision of the estimates increases with sample size; *SI Appendix*, Fig. S8 *B–D*).

Drivers of Community Trajectories. To test whether community temporal dynamics reflect climate exposure, we modeled CTI or CFI trajectories (β-coefficients) separately as a function of the trends in water temperature (trend T_{max}) or streamflow (trend Q_{max}), respectively. To test for the dual forces of climate and land-use change (14, 19), we included an interaction term with the degree of land use. To test whether the sensitivity of communities to climate exposure mediates community responses, we also included an interaction term with community thermal bias or flow bias. Finally, to test whether diverse communities are more resilient to climate exposure, we included an interaction term with species richness. As with the models developed to assess spatial patterns in CTI and CFI trajectories (see Spatial Patterns in Community Trajectories above), we used linear mixed models with a random effect structure accounting for spatial (hydrographic basin ID) dependencies on the estimated temporal trajectories and using sampling weights (number of census years) to control for different sampling schemes. Note that due to the above-mentioned constraints on data availability of water temperature and streamflow time series, the models were ultimately fitted using slightly reduced datasets (12,435 and 12,261 for CTI and CFI trajectories, respectively). The predictors were standardized to *z* scores (mean = 0, variance = 1) prior to model fitting to allow comparison of the coefficients between predictors that were measured on different scales (69). We fitted all possible models using different combinations of predictors and ranked the models according to their AICc. To account for model selection uncertainty, the direction and magnitude of the effect of the different drivers (effect sizes) and associated 95% confidence intervals were estimated using a model averaging procedure (70). This was performed using a subset of models with $\Delta AICc \leq 4$ from the model with the lowest AICc.

All the analyses were performed using the computing environment R (71) using the packages *Epi*, *lattice*, *lme4*, *lmerTest*, *MuMIn*, *RColorBrewer*, *rgbif*, *raster*, *rgdal*, and *scales*.

Data Availability. The fish abundance time series data are available from the RivFishTIME database (53) deposited in iDiv Data Repository (https://doi.org/10.25829/idiv.1873-10-4000; the full list of datasets used in our analyses are presented in *SI Appendix*, Table S3). The water temperature time series data are available from https://doi.org/10.5281/zenodo.3337659 (57), and the streamflow time series data are available from https://doi.org/10.5281/zenodo.1468428 (58). Land cover data are available from the GlobCover2009 database (http://due.esrin.esa.int/page_globcover.php) (61).

ACKNOWLEDGMENTS. We thank Nico Wanders for providing the water temperature data and the ESA GlobCover 2009 Project and the Université Catholique de Louvain as the source of the GlobCover products. We thank all researchers and agencies who contributed their fish abundance time series data—this project would not be possible without their data collection efforts and their generosity in contributing their data: Agència Catalana de l'Aigua; Jaquelini O. Zeni; Lilian Casatti; Luz Jimenez-Segura; Tibor Erős; Jammes Gammon; Department of Environment and Science; Teppo Vehanen; Tapio Sutela; Parks Canada; Keith Gido; David L. Propst; Marsh and Associates; US Environmental Protection Agency; Thiago V. T. Occhi, Jean R. S. Vitule; Akira Terui; Hirokazu Urabe; Iowa Department of Natural Resources; Marco Milardi; Giuseppe Castaldelli; Anna Gavioli; the World Health Organization; Mark Pyron; Keith Gido; Bill McLarney; Jason Meador; Upper Midwest Environmental Sciences Center; William Matthews; Edie Marsh-Matthews; the Murray-Darling Basin Authority; the Minnesota Pollution Control Agency; Montana Fish, Wildlife & Parks; US Geological Survey; UK Environmental Agency; North Carolina Department of Environmental Quality; Rafael P. Leitão; Paulo S. Pompeu; Gilberto N. Salvador; Christopher Taylor; Okavango Research Institute; Office Francais de la Biodiversite; Oklahoma Water Resources Board; Agencia Vasca del Agua; Angelo A. Agostinho; Stephen Davenport; Renato B. Dala-Corte; Fernando G. Becker; Vincent Resh; Toronto and Region Conservation Authority; United States Fish and Wildlife Service; Jerome A. Stefferud; Swedish University of Agricultural Sciences; Emili García-Berthou;

Seiji Miyazono; John Rinne; Gerlinde Van Thuyne; Montgomery County; Tennessee Valley Authority; Regional Aquatics Monitoring Program; Ohio Environmental Protection Agency; National Institute of Water and Atmospheric Research; and the Metropolitan Water Reclamation District of Greater Chicago. A.R. was supported by USDA National Institute of Food and Agriculture Grant NC-1189 and by the University of California, Berkeley new faculty start-up funds.

1. J. Lenoir *et al*., Species better track climate warming in the oceans than on land. *Nat. Ecol. Evol.* **4**, 1044–1059 (2020).
2. L. H. Antão *et al*., Temperature-related biodiversity change across temperate marine and terrestrial systems. *Nat. Ecol. Evol.* **4**, 927–933 (2020).
3. A. J. Reid *et al*., Emerging threats and persistent conservation challenges for freshwater biodiversity. *Biol. Rev. Camb. Philos. Soc.* **94**, 849–873 (2019).
4. J. H. Knouft, D. L. Ficklin, The potential impacts of climate change on biodiversity in flowing freshwater systems. *Annu. Rev. Ecol. Evol. Syst.* **48**, 111–133 (2017).
5. F. Pletterbauer, A. Melcher, W. Graf, "Climate change impacts in riverine ecosystems" in *Riverine Ecosystem Management*, S. Schmutz, J. Sendzimir, Eds. (Springer International Publishing, Cham, 2018), pp. 203–223.
6. D. Tickner *et al*., Bending the curve of global freshwater biodiversity loss: An emergency recovery plan. *Bioscience* **70**, 330–342 (2020).
7. L. Crozier, R. W. Zabel, Climate impacts at multiple scales: Evidence for differential population responses in juvenile chinook salmon. *J. Anim. Ecol.* **75**, 1100–1109 (2006).
8. M. Floury, P. Usseglio-Polatera, M. Ferreol, C. Delattre, Y. Souchon, Global climate change in large European rivers: Long-term effects on macroinvertebrate communities and potential local confounding factors. *Glob. Change Biol.* **19**, 1085–1099 (2013).
9. K. R. Mustonen *et al*., Thermal and hydrologic responses to climate change predict marked alterations in boreal stream invertebrate assemblages. *Glob. Change Biol.* **24**, 2434–2446 (2018).
10. N. Wanders, M. T. H. van Vliet, Y. Wada, M. F. P. Bierkens, L. P. H. van Beek, High-resolution global water temperature modeling. *Water Resour. Res.* **55**, 2760–2778 (2019).
11. D. L. Ficklin, J. T. Abatzoglou, S. M. Robeson, S. E. Null, J. H. Knouft, Natural and managed watersheds show similar responses to recent climate change. *Proc. Natl. Acad. Sci. U.S.A.* **115**, 8553–8557 (2018).
12. K. Chen, J. D. Olden, Threshold responses of riverine fish communities to land use conversion across regions of the world. *Glob. Change Biol.* **26**, 4952–4965 (2020).
13. T. Termaat *et al*., Distribution trends of European dragonflies under climate change. *Divers. Distrib.* **25**, 936–950 (2019).
14. A. Staudt *et al*., The added complications of climate change: Understanding and managing biodiversity and ecosystems. *Front. Ecol. Environ.* **11**, 494–501 (2013).
15. S. R. Carpenter, E. H. Stanley, M. J. Vander Zanden, State of the world's freshwater ecosystems: Physical, chemical, and biological changes. *Annu. Rev. Environ. Resour.* **36**, 75–99 (2011).
16. K. T. Tuff, T. Tuff, K. F. Davies, A framework for integrating thermal biology into fragmentation research. *Ecol. Lett.* **19**, 361–374 (2016).
17. P. Opdam, D. Wascher, Climate change meets habitat fragmentation: Linking landscape and biogeographical scale levels in research and conservation. *Biol. Conserv.* **117**, 285–297 (2004).
18. I. P. Vaughan, N. J. Gotelli, Water quality improvements offset the climatic debt for stream macroinvertebrates over twenty years. *Nat. Commun.* **10**, 1956 (2019).
19. L. O. Frishkoff *et al*., Climate change and habitat conversion favour the same species. *Ecol. Lett.* **19**, 1081–1090 (2016).
20. J. J. Williams, A. E. Bates, T. Newbold, Human-dominated land uses favour species affiliated with more extreme climates, especially in the tropics. *Ecography* **43**, 391–405 (2020).
21. M. Mimura *et al*., Understanding and monitoring the consequences of human impacts on intraspecific variation. *Evol. Appl.* **10**, 121–139 (2016).
22. R. Froese, J. Schilling, The nexus of climate change, land use, and conflicts. *Curr. Clim. Change Rep.* **5**, 24–35 (2019).
23. L. L. Thurman *et al*., Persist in place or shift in space? Evaluating the adaptive capacity of species to climate change. *Front. Ecol. Environ.* **18**, 520–528 (2020).
24. M. Pacifici *et al*., Assessing species vulnerability to climate change. *Nat. Clim. Chang.* **5**, 215–224 (2015).
25. R. D. Stuart-Smith, G. J. Edgar, N. S. Barrett, S. J. Kininmonth, A. E. Bates, Thermal biases and vulnerability to warming in the world's marine fauna. *Nature* **528**, 88–92 (2015).
26. T. Elmqvist *et al*., Response diversity, ecosystem change, and resilience. *Front. Ecol. Environ.* **1**, 488–494 (2003).
27. M. T. Burrows *et al*., Ocean community warming responses explained by thermal affinities and temperature gradients. *Nat. Clim. Chang.* **9**, 959–963 (2019).
28. S. Yachi, M. Loreau, Biodiversity and ecosystem productivity in a fluctuating environment: The insurance hypothesis. *Proc. Natl. Acad. Sci. U.S.A.* **96**, 1463–1468 (1999).
29. M. McLean *et al*., Trait structure and redundancy determine sensitivity to disturbance in marine fish communities. *Glob. Change Biol.* **25**, 3424–3437 (2019).
30. V. Devictor *et al*., Differences in the climatic debts of birds and butterflies at a continental scale. *Nat. Clim. Chang.* **2**, 121–124 (2012).
31. W. W. L. L. Cheung, R. Watson, D. Pauly, Signature of ocean warming in global fisheries catch. *Nature* **497**, 365–368 (2013).
32. A. E. Bates *et al*., Resilience and signatures of tropicalization in protected reef fish communities. *Nat. Clim. Chang.* **4**, 62–67 (2014).
33. J. H. Thorp, M. C. Thoms, M. D. Delong, The riverine ecosystem synthesis: Biocomplexity in river networks across space and time. *River Res. Appl.* **22**, 123–147 (2006).
34. L. B. Leopold, T. J. Maddock, "The hydraulic geometry of stream channels and some physiographic implications" in *USGS Professional Paper* (U.S. Government Printing Office, Washington, DC, 1953), 252.
35. M. Huet, Profiles and biology of western European streams as related to fish management. *Trans. Am. Fish. Soc.* **88**, 155–163 (1959).
36. S. R. Strachan, E. T. Chester, B. J. Robson, Freshwater invertebrate life history strategies for surviving desiccation. *Springer Sci. Rev.* **3**, 57–75 (2015).
37. A. Dai, T. Qian, K. E. Trenberth, J. D. Milliman, Changes in continental freshwater discharge from 1948 to 2004. *J. Clim.* **22**, 2773–2792 (2009).
38. L. Comte, L. Buisson, M. Daufresne, G. Grenouillet, Climate-induced changes in the distribution of freshwater fish: Observed and predicted trends. *Freshw. Biol.* **58**, 625–639 (2013).
39. J. Radinger *et al*., The future distribution of river fish: The complex interplay of climate and land use changes, species dispersal and movement barriers. *Glob. Change Biol.* **23**, 4970–4986 (2017).
40. J. McHenry, H. Welch, S. E. Lester, V. Saba, Projecting marine species range shifts from only temperature can mask climate vulnerability. *Glob. Change Biol.* **25**, 4208–4221 (2019).
41. E. H. Sutanudjaja *et al*., PCR-GLOBWB 2: A 5 arcmin global hydrological and water resources model. *Geosci. Model Dev.* **11**, 2429–2453 (2018).
42. D. Bowler, K. Böhning-Gaese, Improving the community-temperature index as a climate change indicator. *PLoS One* **12**, e0184275 (2017).
43. L. Comte, J. D. Olden, Climatic vulnerability of the world's freshwater and marine fishes. *Nat. Clim. Chang.* **7**, 718–722 (2017).
44. T. Oberdorff *et al*., Global and regional patterns in riverine fish species richness: A review. *Int. J. Ecol.* **2011**, 1–12 (2011).
45. M. J. Troia, A. L. Kaz, J. C. Niemeyer, X. Giam, Species traits and reduced habitat suitability limit efficacy of climate change refugia in streams. *Nat. Ecol. Evol.* **3**, 1321–1330 (2019).
46. T. Oberdorff *et al*., How vulnerable are Amazonian freshwater fishes to ongoing climate change? *J. Appl. Ichthyology* **31**, 4–9 (2015).
47. D. E. Bowler *et al*., Mapping human pressures on biodiversity across the planet uncovers anthropogenic threat complexes. *People Nat.* **2**, 380–394 (2020).
48. A. C. Hughes, Understanding the drivers of Southeast Asian biodiversity loss. *Ecosphere* **8**, e01624 (2017).
49. S. M. Prober *et al*., Shifting the conservation paradigm - a synthesis of options for renovating nature under climate change. *Ecol. Monogr.* **89**, e01333 (2019).
50. B. J. McGill, M. Dornelas, N. J. Gotelli, A. E. Magurran, Fifteen forms of biodiversity trend in the Anthropocene. *Trends Ecol. Evol.* **30**, 104–113 (2015).
51. C. Waldock, M. Dornelas, A. E. Bates, Temperature-driven biodiversity change: Disentangling space and time. *Bioscience* **68**, 873–884 (2018).
52. M. Palmer, A. Ruhi, Linkages between flow regime, biota, and ecosystem processes: Implications for river restoration. *Science* **365**, eaaw2087 (2019).
53. L. Comte *et al*., RivFishTIME: A global database of fish time-series to study global change ecology in riverine systems. *Glob. Ecol. Biogeogr.* **30**, 38–50 (2021).
54. R. Froese, D. Pauly, FishBase. https://www.fishbase.se/. Accessed 2 December 2019.
55. B. Lehner, K. Verdin, A. Jarvis, New global hydrography derived from spaceborne elevation data. *Eos (Wash. D.C.)* **89**, 93 (2008).
56. S. Linke *et al*., Global hydro-environmental sub-basin and river reach characteristics at high spatial resolution. *Sci. Data* **6**, 283 (2019).
57. N. Wanders *et al*., Global Monthly Water Temperature Dataset, Derived from Dynamical 1-D Water-Energy Routing Model (DynWat) at 10 km Spatial Resolution (Version 1.1, 2018). *Zenodo*:https://doi.org/10.5281/zenodo.3337659. Accessed 15 July 2019.
58. N. Wanders *et al*., Global Monthly Discharge Dataset, Derived from Dynamical 1-D Water-Energy Routing Model (DynWat) at 10 km Spatial Resolution (Version 1.0, 2018). *Zenodo*:https://doi.org/10.5281/zenodo.1468428. Accessed 15 July 2019.
59. L. S. Beesley *et al*., Juvenile fish response to wetland inundation: How antecedent conditions can inform environmental flow policies for native fish. *J. Appl. Ecol.* **51**, 1613–1621 (2014).
60. M. J. Kennard, J. D. Olden, A. H. Arthington, B. J. Pusey, N. L. Poff, Multi-scale effects of flow regime and habitat and their interaction on fish assemblage structure in eastern Australia. *Can. J. Fish. Aquat. Sci.* **64**, 1346–1359 (2007).
61. ESA and UCLouvain, Global land cover (GlobCover 2009 Version 2.3). http://due.esrin.esa.int/page_globcover.php. Accessed 25 July 2019.
62. K. K. Goldewijk, N. Ramankutty, "Land use changes during the past 300 years" in *Land Use, Land Cover and Soil Sciences*, W. H. Verheye, Ed. (Encyclopedia of Life Support Systems (EOLSS) Publishers, Oxford, UK, 2004), pp. 147–168.
63. S. Chamberlain *et al*., rgbif: Interface to the Global Biodiversity Information Facility API (Version 1.3.0, R Package, 2019). https://CRAN.R-project.org/package=rgbif. Accessed 22 November 2019.
64. C. Ouellet Dallaire, B. Lehner, R. Sayre, M. Thieme, A multidisciplinary framework to derive global river reach classifications at high spatial resolution. *Environ. Res. Lett.* **14**, 024003 (2019).
65. C. H. Graham, R. J. Hijmans, A comparison of methods for mapping species ranges and species richness. *Glob. Ecol. Biogeogr.* **15**, 578–587 (2006).
66. IUCN, The IUCN Red List of Threatened Species (Version 2019-3, 2017). https://www.iucnredlist.org. Accessed 5 July 2019.
67. M. Kalyuzhny *et al*., Temporal fluctuation scaling in populations and communities. *Ecology* **95**, 1701–1709 (2014).
68. D. Bates, M. Mächler, B. Bolker, S. Walker, Fitting linear mixed-effects models using lme4. *J. Stat. Softw.* **67**, 1–51 (2015).
69. A. Gelman, J. Hill, *Data Analysis Using Regression and Multilevel/Hierarchical Models* (Cambridge University Press, New York, 2007).
70. J. B. Johnson, K. S. Omland, Model selection in ecology and evolution. *Trends Ecol. Evol.* **19**, 101–108 (2004).
71. R Development Core Team, R: A Language and Environment for Statistical Computing (Version.4.0.3, 2020).